

Modulation of the fluorescence yield in heliobacterial cells by induction of charge recombination in the photosynthetic reaction center

Kevin E. Redding · Iosifina Sarrou ·
Fabrice Rappaport · Stefano Santabarbara ·
Su Lin · Kiera T. Reifschneider

Received: 3 September 2013 / Accepted: 25 November 2013 / Published online: 7 December 2013
© Springer Science+Business Media Dordrecht 2013

Abstract Heliobacteria contain a very simple photosynthetic apparatus, consisting of a homodimeric type I reaction center (RC) without a peripheral antenna system and using the unique pigment bacteriochlorophyll (BChl) *g*. They are thought to use a light-driven cyclic electron transport pathway to pump protons, and thereby phosphorylate ADP, although some of the details of this cycle are yet to be worked out. We previously reported that the fluorescence emission from the heliobacterial RC *in vivo* was increased by exposure to actinic light, although this variable fluorescence phenomenon exhibited very different characteristics to that in oxygenic phototrophs (Collins et al. 2010). Here, we describe the underlying mechanism behind the variable fluorescence in heliobacterial cells. We find that the ability to stably photobleach P₈₀₀, the primary donor of the RC, using brief flashes is inversely correlated to the variable fluorescence. Using pump-probe spectroscopy in the nanosecond timescale, we found that illumination of cells with bright light for a few seconds put them

in a state in which a significant fraction of the RCs underwent charge recombination from P₈₀₀⁺A₀⁻ with a time constant of ~20 ns. The fraction of RCs in the rapidly back-reacting state correlated very well with the variable fluorescence, indicating that nearly all of the increase in fluorescence could be explained by charge recombination of P₈₀₀⁺A₀⁻, some of which regenerated the singlet excited state. This hypothesis was tested directly by time-resolved fluorescence studies in the ps and ns timescales. The major decay component in whole cells had a 20-ps decay time, representing trapping by the RC. Treatment of cells with dithionite resulted in the appearance of a ~18-ns decay component, which accounted for ~0.6 % of the decay, but was almost undetectable in the untreated cells. We conclude that strong illumination of heliobacterial cells can result in saturation of the electron acceptor pool, leading to reduction of the acceptor side of the RC and the creation of a back-reacting RC state that gives rise to delayed fluorescence.

Electronic supplementary material The online version of this article (doi:10.1007/s11120-013-9957-4) contains supplementary material, which is available to authorized users.

K. E. Redding (✉) · I. Sarrou · S. Santabarbara · S. Lin ·
K. T. Reifschneider
Department of Chemistry and Biochemistry, Arizona State
University, 1711 S. Rural Rd., Tempe, AZ 85287-1604, USA
e-mail: kevin.redding@asu.edu

K. E. Redding · F. Rappaport · S. Santabarbara
Institut de Biologie Physico-Chimique, UMR 7141 CNRS-Univ.
P. et M. Curie, 75005 Paris, France

Present Address:

S. Santabarbara
Institute of Biophysics, Consiglio Nazionale delle Ricerche,
Via G. Celoria 26, 20133 Milan, Italy

Keywords Heliobacteria · Fluorescence ·
Type I reaction center

Introduction

Variable fluorescence has been a very useful tool for analysis of photosynthetic electron flow and physiology of photosynthetic organisms. When photosynthetic pigments are excited by absorption of a photon, there are four possible fates for the excited state: photochemistry, fluorescence, intersystem crossing (to a triplet state), or conversion to heat. When photosynthetic systems are operating efficiently, photochemistry dominates and the fluorescence yield is low. When these systems become

photochemically less efficient, for a variety of reasons, energy is emitted as fluorescence or heat. Although the latter is dominant, fluorescence is much easier to detect, and has been widely used as a measure of the efficiency of photochemical processes in photosynthesis.

There are two main mechanisms for the increase in fluorescence (or variable fluorescence) observed when photochemistry becomes inefficient. If charge separation is inhibited, either because the primary donor is oxidized or because the free energy of charge separation has been raised due to the accumulation of a reduced downstream cofactor, then there will be an increase in fluorescence from the equilibrated antenna. If charge separation still occurs but further electron transfer (ET) is inhibited, then the charge-separated state can recombine to the ground state, excited triplet state, or excited singlet state, the last of which would lead to fluorescence emission. Because the lifetime of recombination from the initial charge-separated state is typically in the tens of nanoseconds, while the lifetime of the excited state in the antenna is a few nanoseconds, and the emission of fluorescence by the second mechanism will be delayed relative to the emission by the first.

In oxygenic phototrophs, the majority of fluorescence is emitted from the antenna of Photosystem II (PS2), with only ~5–20 % of emission originating from Photosystem I (PS1), depending on the PS2 photochemical efficiency and on the emission wavelength (Samson et al. 1999). This is due to several reasons. First, the PS2 fluorescence yield is controlled primarily by the redox state of the electron acceptor Q_A , which is a plastoquinone molecule. When Q_A is oxidized, the photochemical yield is high (typically ~80–85 %) and the fluorescence yield is low (so called F_0 level). The average lifetime of excited state decay, under conditions of oxidized Q_A is ~200 ps (Hodges and Moya 1986; Holzwarth et al. 1985; Broess et al. 2006; Caffarri et al. 2011), and the $P_{680}^+Pheo^-$ radical is efficiently depopulated due to ET from $Pheo^-$ to Q_A . When Q_A is reduced, the yield of primary charge separation can be decreased, due to the increase in free energy of the $P_{680}^+Pheo^-$ radical pair in the presence of the negative charge of Q_A^- . Moreover, since ET from $Pheo^-$ to Q_A^- is slow, the charge-separated state recombines quickly repopulating the reaction center excited state, which is equilibrated with the antenna bed (Schatz et al. 1988; Engelmann et al. 2005; Miloslavina et al. 2006). Under these conditions, the fluorescence yield is high (F_M conditions) and the average lifetime of the singlet excited state is ~1–1.5 ns (Hodges and Moya 1986; Moya et al. 1986; Roelofs et al. 1992), corresponding to an increase in steady-state emission of four to fivefold compared to when Q_A is oxidized and the centers are fully active. Thus, continuous actinic light of sufficient intensity will induce a rise in fluorescence as the plastoquinone pool becomes

reduced by the action of PS2, resulting in photoaccumulation of Q_A^- . This variable fluorescence can be used to estimate the efficiency of PS2 (Buttler 1978; Duysens 1978), and many techniques have taken advantage of this fact.

The fluorescence emission of PS1, at room temperature, is generally much weaker than that of PS2, being characterized by an average lifetime of ~20–40 ps (Gobets and van Grondelle 2001; Ihalainen et al. 2005; Slavov et al. 2008; Engelmann et al. 2006; Wientjes et al. 2011), although some variation across the emission band with maximal values of ~60–80 ps been also observed in the long wavelength emission tail (Engelmann et al. 2006; Galka et al. 2012; Jennings et al. 2013). Moreover, the lifetime appears to be relatively insensitive to the redox state of ET cofactors. A possible explanation resides in the fact that the analog of Q_A^- in PS1 is a phyllosemiquinone (PhQ^- , also called A_1^-) which is difficult to accumulate, as there are 3 [4Fe–4S] clusters (F_X , F_A , and F_B) beyond this ET intermediate. The lifetime of PhQ^- in PS1 is 10–300 ns (Sétif and Brettel 1993; Guergova-Kuras et al. 2001; Santabarbara et al. 2005; Rappaport et al. 2006), while the lifetime of Q_A^- in PS2 is at least ~300 μ s and increases to the timescale of seconds when forward ET from Q_A is blocked (Bowes and Crofts 1980). Even closed PS1 RCs (in which P_{700} is oxidized) can quench excitations in 20–30 ps (Hastings et al. 1994; White et al. 1996; Byrdin et al. 2000). This has recently been explained by the fact that primary charge separation occurs within the *ec2/ec3* Chl pairs in PS1 and the charge-separated state is further stabilized by ET from P_{700} to the oxidized *ec2* Chl (Müller et al. 2003, 2010; Holzwarth et al. 2006). When P_{700} is oxidized, the first radical pair can be formed (albeit with somewhat lower yield due to the positive charge on P_{700}), but it then decays in the picosecond timescale to the ground state, effectively quenching fluorescence (Giera et al. 2010). Illumination of PS1 particles or PS1-containing membranes in the presence of dithionite results in an increase in steady-state fluorescence (Ikegami 1976; Tripathy et al. 1984; Kleinherenbrink et al. 1994), and this has been explained as resulting from “delayed fluorescence” in PS1 RCs in which the quinone was doubly reduced to a quinol. In that case, formation of the $P_{700}^+A_0^-$ radical pair would be followed by charge recombination of this state, some of which would regenerate the singlet excited state (leading to fluorescence), since forward ET is blocked. The appearance of a 35-ns fluorescence decay component, which matches the decay time of the $P_{700}^+A_0^-$ radical pair, is consistent with this interpretation (Kleinherenbrink et al. 1994).

Anoxygenic phototrophic bacteria, which make use of a single reaction center, exhibit the phenomenon of variable fluorescence. It was established some time ago that fluorescence in purple proteobacteria, which use a type 2 RC, is

primarily determined by the state of the secondary electron acceptor, Q_A (Clayton 1967; Reed et al. 1969; Zankel et al. 1968; van Grondelle et al. 1978). The purple bacterial RC is somewhat special, in that the special pair and primary donor (P_{865}) has an absorption maximum significantly red-shifted compared to the other RC and antenna pigments, making it responsible for the lowest energy emission. Oxidation of P_{865} results in low fluorescence, while reduction of Q_A results in a ~ 5 -fold increase in fluorescence (Reed et al. 1969; Zankel et al. 1968). The origin of variable fluorescence in purple bacteria is now interpreted, as in the case of oxygenic PS2, in terms of photochemical quenching by the “open” (oxidized Q_A) centers, disappearing as Q_A^- is reduced, thereby attaining a maximal level.

Variable fluorescence was also observed in anoxygenic bacteria utilizing type 1 RCs, such as the green sulfur bacteria (Clayton 1965). In *Chlorobaculum tepidum*, fluorescence emission from the bacteriochlorophyll (BChl) *a* of the FMO protein linking the chlorosome to the RC was seen to increase after a brief illumination, although fluorescence from the chlorosome itself was unchanged (Hohmann-Marriott and Blankenship 2007). Variable fluorescence has also recently been observed in *Heliobacterium modesticaldum* (Collins et al. 2010).

The photosynthetic apparatus of *Heliobacteria* is much simpler, as the only pigment-binding protein that they possess is the RC itself. Not only do they lack any peripheral antenna system, but the heliobacterial RC (HbRC) itself has a very small core antenna consisting of only 18 BChl *g* in *H. modesticaldum* (Heinrickel et al. 2006; Sarrou et al. 2012). The HbRC of this organism is composed of two BChl *g'* (special pair P_{800}), two BChl *g*, and two 8^1 -OH-Chl *a_F* (A_0 ; (Sarrou et al. 2012; Chauvet et al. 2013), as shown before in other species (Amesz 1995). The physiology of heliobacterial cells is not yet known in detail. A lipid-linked cytochrome *c* serves as the carrier between the cyt b_6c complex and the HbRC and that cyt c_{553} can re-reduce P_{800}^+ of the HbRC in ~ 1 ms at room temperature (this work), likely faster at higher temperatures (Oh-oka et al. 2002). Cyt c_{553} is reduced by the cytochrome b_6c complex, which resembles a hybrid between the cyt b_6f and cyt bc_1 complexes. It has a split cyt b_6 with the attached heme c_i near the cyt b_H , but uses a diheme cyt c (*i.e.* neither cyt f nor cyt c_1) as an intermediate between the Rieske FeS cluster and the mobile cyt c_{553} (Ducluzeau et al. 2008). The pool quinone is menaquinone (MQ), primarily MQ-9 with smaller amounts of MQ-8 (Hiraishi 1989). An average of 1.5–1.6 MQ per RC are found in purified RCs from this species (Sarrou et al. 2012), leading to the expectation of two quinones per RC, as in PS1. However, participation of MQ in ET between P_{800} and F_X is still controversial. Although a radical attributed to a semiquinone was detected by X-band EPR (Muhiuddin et al.

1999; Miyamoto et al. 2008), time-resolved optical spectroscopy (Lin et al. 1995; Brettel et al. 1998), and transient EPR (van der Est et al. 1998) failed to observe the semiquinone as an ET intermediate. Moreover, extraction of menaquinone from heliobacterial membranes had no effect upon forward ET (Kleinherenbrink et al. 1993).

Another way in which the HbRC is different from PS1 is the presence or absence of the terminal F_A/F_B clusters. In PS1, these are bound by the extrinsic PsaC subunit, which is bound very tightly to the PsaA/PsaB heterodimer (Jaganathan and Golbeck 2009a, b). The PshB polypeptide was found associated with the HbRC purified by sucrose density gradients. Like PsaC, it is a bacterial-type ferredoxin harboring two [4Fe–4S] clusters (Heinrickel et al. 2005, 2007), and PshB was therefore expected to play the same role as PsaC. However, this interpretation now seems unlikely in light of recent discoveries. Firstly, it was surprisingly easy to remove PshB from the HbRC core, requiring only 0.5 NaCl (Heinrickel et al. 2005), while 7 M urea is required to remove PsaC from PS1 (Parrett et al. 1989). Secondly, there are two similar genes next to each other on the genome encoding paralogous gene products, PshB1 and PshB2 (Romberger et al. 2010), which is difficult to reconcile with the idea that one or both is a subunit. Lastly, it has recently been shown that the core HbRC lacking PshB could reduce cyanobacterial flavodoxin in a light-dependent manner and that the addition of either PshB1 or PshB2 inhibited rather than accelerated this reaction (Romberger and Golbeck 2012), consistent with the idea that they were competing for electrons from F_X . Thus, the PshB1 and PshB2 polypeptides are most likely mobile electron carriers, acting to re-oxidize F_X and then dissociate from the HbRC. This would imply that the PsaA homodimer is the functional HbRC and that the F_X cluster is the terminal electron acceptor, which is quite different from PS1.

When illuminated, fluorescence emission from heliobacterial cells does not start to rise until after at least 10–100 ms, depending on the temperature and the intensity of the actinic light (Collins et al. 2010). Variable fluorescence in heliobacteria could be blocked by the addition of oxidants like ferricyanide, and enhanced by addition of low-potential reductants like dithionite. It was also inhibited by reagents that slow re-reduction of P_{800}^+ or that reoxidize the terminal FeS clusters of the HbRC. These characteristics led to a model in which exhaustion of the electron acceptor pool, but not the donor pool, led to accumulation of reduced FeS clusters in the HbRC. Once the F_X cluster was reduced, subsequent excitation and charge separation would lead to production of the $P_{800}^+A_0^-F_X^-$ state, followed by charge recombination and emission of delayed fluorescence. In this work, we have examined the HbRC by transient absorption spectroscopy in the ns timescale to test this model. We find that illumination of heliobacterial cells for a second or so produces in high yield

an HbRC state in which the $P_{800}^+A_0^-$ state is generated and subsequently recombines. The fraction of back-reacting HbRCs correlates very well with the variable fluorescence yield. Moreover, analysis of the fluorescence emission by the time-correlated single photon counting (TCSPC) technique demonstrates the appearance of an 18-ns fluorescence decay component when cells are exhibiting variable fluorescence. The spectrum of this emission is consistent with emission from the HbRC antenna.

Materials and methods

Growth of *Heliobacterium modesticaldum* cells

Cells were grown in PYE medium within sealed 100-mL Wheaton bottles. Typically, 100 mL of medium was inoculated with 1 mL of culture and incubated 16–24 h under illumination in a water bath at 46–48 °C. Unless otherwise stated, cells were loaded into cuvettes using a stream of N_2 gas to transfer them anoxically from the bottle into the cuvet via tubing that had been pre-flushed for over 15 min.

LED flash fluorescence and transient absorption spectroscopy in ms-sec timescale

This was performed using a JTS-10 LED kinetic spectrometer (Bio-Logic, Grenoble, France). Fluorescence from BChl *g* in living cells was monitored using a 10- μ s (excitation) measuring pulse at 420 nm, and detected through a long-pass filter in front of the detectors allowing emission of wavelengths >780 nm to be measured. Actinic illumination was provided by a battery of LEDs, whose intensity was adjusted electronically from 10 to 1,700 μ mol photons $m^{-2} s^{-1}$. Collection of transient absorption and fluorescence data was during a 200- μ s period of darkness, so that the actinic light would not interfere with the measurement. The protocol also involved giving 40-ms pulses of bright (4,300 μ mol photons $m^{-2} s^{-1}$) actinic light every 2 s to assess the maximal fluorescence level attainable (or the redox state of ET intermediates in absorption experiments), which was sampled 200 μ s after the 40-ms pulse. The optical path length was 1 cm in all cases.

Laser-flash pump-probe spectroscopy in ns-ms timescale

This was performed using a home-built double-flash spectrometer (Béal et al. 1999). Actinic light was provided by a red laser diode with emission centered at 690 nm. The apparatus was modified to allow fluorescence detection by inserting the following filters between the cuvet and the

detector: RG790, RG810, and two RG9 filters. The excitation light used for fluorescence measurements was a 6-ns flash centered at 425 nm. The $t = 0$ time was defined as the delay between the pump and probe pulses that yielded 50 % of the maximal signal associated with P_{800} oxidation.

Picosecond fluorescence spectroscopy

Cell culture was loaded into an air-tight cuvet inside an anaerobic chamber; for strongly reducing conditions, sodium dithionite was added to a final concentration of 50 mM. Fluorescence decay kinetics were measured using the time-correlated single photon counting (TCSPC) technique (Liddell et al. 2008). The excitation source was a titanium sapphire (Ti:S) laser (Spectra-Physics, Millennia pumped Tsunami) with a 130-fs pulse duration operated at 82 MHz. The laser output was tuned to 760 nm and sent through a pulse selector (Spectra Physics, Model 3980) to operate at a repetition rate of 4 MHz with an average power of 2 mW (i.e. $\sim 2 \times 10^8$ photons per pulse). The area of the laser beam was a circular spot ~ 0.5 mm in diameter. Fluorescence emission was collected at a 90° geometry and detected using a double-grating monochromator (Jobin-Yvon, Gemini-180) and a microchannel plate photomultiplier tube (Hamamatsu R3809U-50). Fluorescence was detected at the magic angle (54.7°) relative to the polarization of the excitation pulses. Data acquisition was done using a single photon counting card (Becker-Hickl, SPC-830). The instrument response function was 40 ps at FWHM. In each experiment, excitation power was varied to ensure that annihilation was not an issue. Data analysis was carried out using local written software ASUFIT (URL: www.public.asu.edu/~laserweb/asufit/asufit.html). Kinetic decay curves collected over the entire wavelength region were fit globally with a sum of exponential decay model using equation $F(\lambda) = \sum_i A_i(\lambda)e^{-t/\tau_i}$. The amplitude as a function of wavelength ($A_i(\lambda)$) for each decay lifetime, τ_i , is presented as the decay associated spectrum (DAS).

Results

Transient absorption: reduction of P_{800}^+ by cyt *c* and re-reduction of cyt *c*

We measured kinetics of absorbance changes in the 390–600 nm spectral range produced by 5- μ s red flashes in living *H. modesticaldum* cells. As the results obtained were very similar to what had been seen previously in *Helio-bacillus mobilis* cells (Kramer et al. 1997; Nitschke et al. 1995), they will be discussed only briefly here. (See the Supplemental Information and Fig. S1 for more details.)

The immediate flash-induced bleaching of the BChl *g* Soret band (400 nm) and Q_y band (572 nm) attributed to oxidation of P_{800} decays with a time constant of ~ 1 ms, concomitant with the rise of new bleaching bands attributed to oxidation of cytochrome (cyt) c_{553} at ~ 420 nm (Soret), ~ 525 nm (β), and 553 nm (α). These bleachings are the same as seen previously with the cyt c_{553} from *H. gestii* (Albert et al. 1998), and this protein is well conserved between the two species (Fig. S2) (Albert et al. 1998; Oh-oka et al. 2002). The rate of this reaction increased as the temperature was raised (data not shown), as was seen previously in whole cells of *H. gestii* (Oh-oka et al. 2002), but at room temperature we saw no evidence for a faster kinetic component or for a slowing of this rate between early and late log cultures (Fig. S3). Cyt c_{553} is re-reduced with an apparent time constant of ~ 150 ms, which is attributed to the reduction of the di-heme cyt *c* by the Rieke FeS cluster within the cyt b_{6c} complex. This is accompanied by net oxidation of a cytochrome *b*, consistent with the operation of a Q-cycle in the heliobacterial cyt b_{6c} complex. (See the Supplemental Information for more details.) Thus, the details of ET from the cyt b_{6c} complex to the HbRC via the membrane-attached cyt c_{553} appear to be very similar between *H. modesticaldum* and previously examined heliobacterial species.

Inverse relationship between stable P_{800}^+ and variable fluorescence

Fluorescence emission from BChl *g* in living cells was monitored using 10- μ s excitation pulses in the blue region (see “Materials and Methods”). As observed earlier with a different type of instrument (Collins et al. 2010), continuous illumination produced an increase in fluorescence, but the rise was strongly dependent upon the intensity of the actinic illumination (Fig. 1a). A bright 40-ms pulse of actinic light was given every 2 s to see if the fluorescence was close to saturation; as can be seen, this was never the case, although saturation was approached at the highest actinic light levels.

Using a similar sequence of flashes, absorbance measurements were performed at 805 nm to measure P_{800} oxidation and at 554 nm to measure cyt *c* oxidation. Without continuous actinic light, the bright pulses were sufficient to obtain transient maximal bleaching signals for both P_{800} and cyt c_{553} (Fig. 1b, c; black traces). As the intensity of the continuous actinic light was increased, the steady-state level of P_{800} bleaching rose, presumably by a partial limitation on the electron donor side. Somewhat unexpectedly, the level of P_{800} bleaching attained immediately after the 40-ms bright pulse became lower as the actinic light was increased. At the highest actinic light level used (1,700 $\mu\text{mol photons m}^{-2} \text{s}^{-1}$), the level of P_{800}

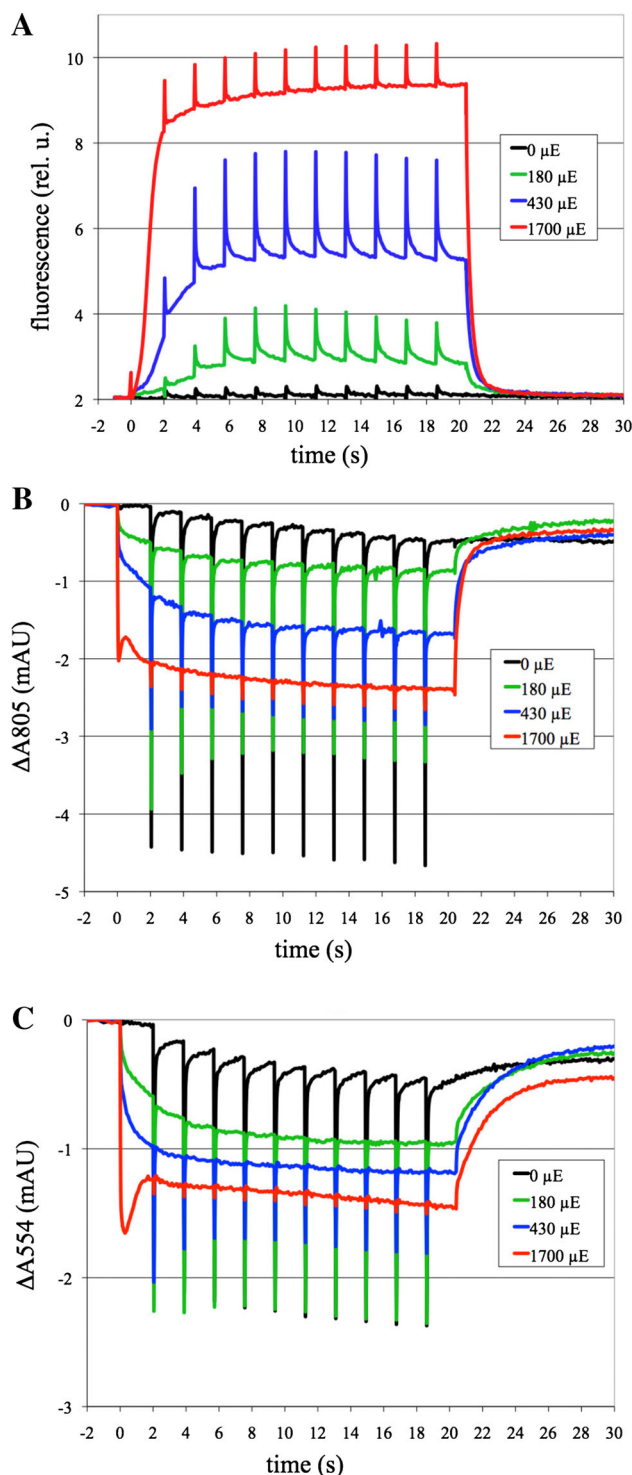


Fig. 1 Fluorescence (a), P_{800} (b), and cyt c_{553} (c) levels during illumination of live *H. modesticaldum* cells. Actinic light was provided by orange LEDs at an intensity of 0 (black), 180 (green), 430 (blue), and 1,700 $\mu\text{mol photons m}^{-2} \text{s}^{-1}$ (red). P_{800} levels were monitored at 805 nm (b) and cyt c_{553} levels were detected at 554 nm (c). Every ~ 2 s, the actinic light was pulsed to 4,300 $\mu\text{mol photons m}^{-2} \text{s}^{-1}$ for 40 ms; the next detection flash was 200 μs after the bright pulse. Illumination was initiated at 0 s and terminated at 20.4 s (Note that all three measurements were made with the same set of cells within a few minutes of each other)

photobleaching produced by the pulse was minimal (Fig. 1b, red trace). This experiment was also run using a saturating 6-ns laser flash to fully oxidize P_{800} , and essentially the same results were obtained (Supplemental Information, Fig. S4), ruling out an artifact specific to the method used to bleach P_{800} .

Since the detection flash was given 200 μ s after the bright 40-ms pulse, an ET event reducing P_{800}^+ faster than that would decrease the observed P_{800} photobleaching (i.e. the oxidation and re-reduction would occur during the spectrometer “dead time”). One possible explanation is that reduction of P_{800}^+ by cyt c_{553} would become faster in cells exposed to continuous high actinic light, due to optimization of ET processes. If this were the case, we would expect to see a similar amount of cyt c_{553} oxidized after each pulse, as cyt c_{553} is re-reduced by the cyt b_6c complex in tens of ms (see above and Supplemental Information). However, the small amounts of P_{800}^+ photobleaching produced by the pulses during high actinic light were matched by correspondingly small amounts of cyt c_{553} photobleaching (Fig. 1c). Thus, the fast reduction of P_{800}^+ in high light must be carried out by another electron donor. This is strengthened by the observation that the steady-state level of P_{800}^+ increased with higher actinic light (Fig. 1b), but not as much as one would expect. (For example, after increasing actinic illumination ~ 4 -fold from 430 to 1,700 μ mol photons $m^{-2} s^{-1}$, the steady-state level of P_{800}^+ increased from ~ 50 % of maximum to only ~ 60 % of maximum).

We found that the level of fluorescence observed was inversely related to the amount of “stable” P_{800} photobleaching observable by this technique. (We operationally define “stable P_{800}^+ ” as enduring longer than 200 μ s.) We have observed this phenomenon under many different conditions, including aging of cultures, addition of exogenous reductants, oxidants, inhibitors, etc. (see Figs. S5 and S6 in the Supplemental Information for some examples). In every case, when the level of P_{800} bleaching produced by a strong pulse of light was low, the fluorescence yield immediately after the pulse was high, and vice versa. We found earlier that a limitation of ET from cyt b_6c and the RC imposed by addition of stigmatellin blocked the fluorescence rise [(Collins et al. 2010); see also Fig. S5b]; this treatment also produced maximal stable P_{800} photobleaching (Fig. S5a). Thus, a limitation on the donor side should lead to a high steady-state level of P_{800}^+ and a low fluorescence state. Since the loss of stable P_{800} photobleaching is not due to rapid reduction by cyt c_{553} (see above), our hypothesis to explain these data is that there must be a limitation on the acceptor side when cells become highly fluorescent. That the electron acceptor pool would become limiting before the donor pool is unexpected; this is

discussed further below (see “Discussion” section). Consistent with this hypothesis, we observed that the addition of dithionite, which should result in reduction of the electron acceptor pool (at least partially), has the effect of increasing the fluorescence yield [(Collins et al. 2010); see also Fig. S6a]. Under these conditions, the yield of stable flash-induced P_{800} photobleaching was decreased (Fig. S6b).

We further hypothesize that this acceptor side limitation will lead to reduction of the FeS cluster(s) of the RC (Collins et al. 2010). If the PshB1/PshB2 polypeptides act as acceptors rather than subunits (see “Introduction”), then they would be part of the reduced acceptor pool. Once PshB had dissociated, F_X^- would be easily photoaccumulated, since charge recombination of $P_{800}^+F_X^-$ (15–20 ms) is much slower than reduction of P_{800}^+ by cyt c_{553} (~ 1 ms). However, even if the PshB polypeptides did not dissociate, the terminal acceptors of the RC would be reduced in a large fraction of centers, if the acceptor pool or the ambient potential was sufficiently reducing. Excitation of RCs in the $P_{800}F_X^-$ state should lead to generation of the $P_{800}^+A_0^-F_X^-$ state, which would be followed by charge recombination in ~ 20 ns (Kleinherenbrink et al. 1991) to either re-generate the P_{800}^* excited state or produce $^3P_{800}$. A certain fraction may also recombine directly to the ground state (i.e. internal conversion). Emission from the singlet excited state would be the source of delayed fluorescence. The fast back-reaction of $P_{800}^+A_0^-$ would preclude observation of P_{800} bleaching driven by the pulse, as it would have decayed long before the measuring flash 200 μ s after the pulse. This hypothesis would provide an explanation for the inverse relationship between stable P_{800} photobleaching and variable fluorescence.

Pump-probe studies of forward and reverse ET from A_0^- in the ns timescale

In order to test this hypothesis, we needed to observe in a direct way the ET reactions taking place within heliobacterial cells in the nanosecond timescale. To do this, we made use of a lab built laser-flash pump-probe spectrometer designed to work with strongly scattering samples (Béal et al. 1999). Fresh heliobacterial cultures were loaded anoxically into air-tight cuvettes, and were dark adapted for at least 1 min before each time course. The rate of ET from A_0 to F_X is ~ 600 ps in the HbRC purified from *H. modesticaldum* (Chauvet et al. 2013), similar to what was seen previously with other species (Neerken and Ames 2001). The earliest spectrum that could be taken (~ 3 ns) should therefore contain contributions from $P_{800}^+A_0^-$ and $P_{800}^+F_X^-$, with the former comprising a very small minority. By 17 ns, one would expect essentially all of the

$P_{800}^+A_0^-$ to have been converted to $P_{800}^+F_X^-$, yielding a ‘pure’ ($P_{800}^+F_X^- - P_{800}F_X$) difference spectrum (Fig. 2). Thus, by performing a subtraction, and assuming that the contribution of $[F_X^- - F_X]$ is minimal in this spectral range, we obtained an $A_0^- - A_0$ difference spectrum (Fig. 2). These two difference spectra are compared in Fig. 2, with the ($P_{800}^+ - P_{800}$) difference spectrum scaled down 15-fold to enable facile comparison. If one assumes that the extinction coefficients of the bleaching band in the Soret region for P_{800} and A_0 are of a similar magnitude, then this implies that $\sim 6\text{--}7\%$ of the HbRCs remain in the $P_{800}^+A_0^-$ state 3 ns after the pump flash. This is surprising, using an estimated rate of ET from A_0 to F_X of $\sim 1.5\text{ ns}^{-1}$, one would predict that only $\sim 1\%$ of $P_{800}^+A_0^-$ would remain at 3 ns after the pump flash. It is possible that this ET event is bi-phasic and that the ultra-fast studies missed a minor component with a slower lifetime of ET. Nevertheless, the ($A_0^- - A_0$) difference spectrum thus obtained is very similar to the one obtained in membrane fragments from *H. mobilis* using ultra-fast pump-probe spectroscopy in the ps timescale (Lin et al. 1995), at least in the region of spectral overlap (400–470 nm); the difference spectrum presented in Fig. 2 is over a much larger spectral range. Comparison of the $P_{800}^+ - P_{800}$ and $A_0^- - A_0$ difference spectra provided us with key wavelengths that were specific for P_{800} (600 nm) or A_0 (580 nm), or that could be used to monitor both (e.g. 460 nm).

The pump-probe system was modified to measure laser-flash-induced absorbance changes while illuminating the cells with a red laser diode (690 nm). At 460 nm, which monitors both P_{800}^+ and A_0^- , a small fraction of the signal

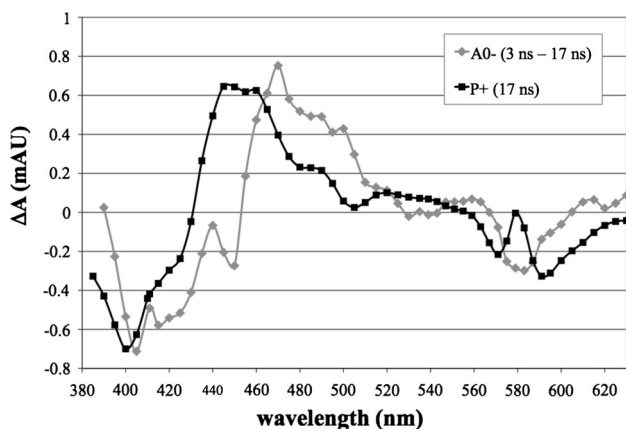


Fig. 2 Comparison of $P_{800}^+ - P_{800}$ (black) and $A_0^- - A_0$ (gray) difference spectra in whole *H. modesticaldum* cells. The black spectrum was obtained 17 ns after the pump flash, and should correspond to the $P_{800}^+ - P_{800}$ difference spectrum. The gray spectrum is the difference between the spectra taken 3 and 17 ns after the pump flash, and should correspond to the $A_0^- - A_0$ difference spectrum (The black spectrum was scaled down by a factor of 15 to facilitate comparison.)

decays within ~ 10 ns in dark-adapted cells, and should thus correspond to the ‘tail’ of A_0^- decay (Fig. 3a). The addition of dithionite and PMS to cells in the dark did not noticeably change the decay kinetics (Fig. 3a and data not shown). However, pre-illumination for a few seconds with red light was sufficient to induce a drastic change in the kinetics. In cells that had been illuminated for 2 s, $>80\%$ of the absorbance change at 460 nm decayed with an apparent time constant of ~ 12 ns. This rate is consistent with charge recombination from the $P_{800}^+A_0^-$ state. Spectra obtained at 3 and 50 ns after the flash demonstrated that most of the charge separation was unstable in cells that had been pre-illuminated in the presence of dithionite and PMS (Fig. 3b). Taking the difference between the two transient spectra allowed us to obtain a spectrum of the fast decaying species, which we assign to ($P_{800}^+A_0^- - P_{800}A_0$). Interestingly, a weighted sum of the ($P_{800}^+ - P_{800}$) and ($A_0^- - A_0$) difference spectra produced a reasonable approximation of the ($P_{800}^+A_0^- - P_{800}A_0$) difference spectrum (Fig. S7), suggesting that, if formed, (${}^3P_{800} - P_{800}$) is hardly detectable in our conditions, consistent with the findings of Vrieze et al. (Vrieze et al. 1998).

Direct correlation of fluorescence increase with back-reaction

We found that, although the presence of dithionite accelerated the induction of a rapidly recombining state, strong actinic light was the only requirement. This is demonstrated in Fig. 4. During each time course of actinic illumination, a saturating single-turnover laser flash was fired every ~ 500 ms, followed by a probe flash after a certain delay (8 ns, 50 ns, 3 μ s, or 1 ms), to assess the stability of charge separation. The initial pump-probe measurement before illumination gave the expected result: only a very small signal attributable to A_0^- was seen at 8 ns, and it had completely decayed by 50 ns (Fig. 4c), while P_{800}^+ did not start to decay until after 3 μ s, and was $\sim 60\%$ gone by 1 ms (Fig. 4a, b).

After illumination commenced, we saw steady-state photobleaching of P_{800} within 100 ms, as assessed by the probe flashes at 600 nm (Fig. 4c). (Note that changes at 460 nm cannot be used to quantify steady-state photobleaching of P_{800} , due to contributions from longer-lived processes, likely including energization of the membrane; data not shown). However, the additional pump flash-induced P_{800} photobleaching was no longer completely stable in the ns time scale. After 500 ms of actinic illumination (at $400\ \mu\text{mol photons m}^{-2}\text{ s}^{-1}$), less than 60% of the P_{800}^+ persisted to 50 ns. After 4 s of illumination, less than 10% of flash-induced charge separation was stable. The decrease of stable P_{800}^+ was paralleled by the increase of A_0^- (transient bleach at 580 nm) seen at 8 ns

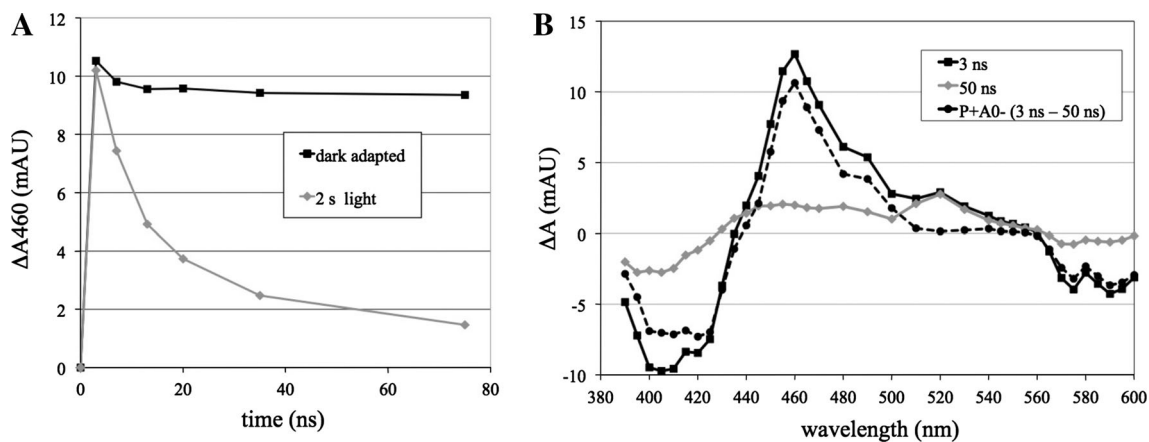


Fig. 3 Time-resolved absorption spectroscopy of *H. modesticaldum* cells treated with 5 mM dithionite and 10 μ M PMS. **a** Kinetics of absorbance changes at 460 nm in cells before (black) or after (gray) illumination for 2 s with red light ($400 \mu\text{mol photons m}^{-2} \text{s}^{-1}$), preceding the actinic laser flash. **b** Transient spectra obtained 3 ns

(black squares) and 50 ns (gray diamonds) after pump flash in *H. modesticaldum* cells treated with dithionite and PMS and pre-illuminated for 2 s with red light. The difference spectrum (dashed) is attributed to $(P_{800}^+A_0^-) - (P_{800}A_0)$

after the pump flash (Fig. 4c). As expected, A_0^- mostly disappeared by 50 ns after the pump flash. The transient flash-induced increase at 460 nm (which monitors both P_{800}^+ and A_0^-) reflects both these changes, in that the magnitude of the transient rise both increased and became less stable during the time course (Fig. 4a).

The rise of the rapidly recombining state seemed reminiscent of the rise of fluorescence seen in the LED instrument. However, the actual actinic light experienced by the cells was not directly comparable between these experiments due to the different optical configuration of the two spectrometers. Since, it is essential to measure both fluorescence and transient absorption with the same set-up, the laser-flash pump/probe system was modified to allow direct comparison of fluorescence and transient absorption intensities. Although it was not possible to perform both measurements at the same time, we could change experiments within a minute, allowing observation of fluorescence rise and transient absorption changes under the exact same conditions. This was more than sufficient, as these time courses were very reproducible for several hours (data not shown).

The combined experiment is shown in Fig. 5 for three different actinic light intensities. The rise in fluorescence mirrored the rise in RCs exhibiting the fast back-reaction. In order to test this correlation more quantitatively, we calculated the fraction of back-reacting RCs at each time point in the three time courses, as well as the variable fluorescence (normalized to the extrapolated maximal fluorescence) at the same time point. These are plotted versus each other in Fig. 5D. The correlation is very good ($R^2 \approx 0.98$). Thus, we can explain virtually all of the variable fluorescence as being due to RCs that are in the fast back-reacting state.

Single photon counting analysis of fluorescence emission from cells

Our working hypothesis is that under strong illumination, the acceptor pool within heliobacterial cells becomes reduced, resulting in the steady-state reduction of the acceptor(s) within the RC. Once, the acceptor from A_0^- within a RC becomes reduced (which we will refer to as 'X'), the RC will be in a closed state ($P_{800}A_0X^-$) leading to rapid recombination after excitation ($P_{800}^+A_0^-X^-$). Although our work here does not identify this acceptor, we think it is likely to be the F_X cluster (see "Discussion" section). Regeneration of the excited state by charge recombination in a fraction of the recombining RCs will result in delayed fluorescence emission from the RC/antenna system. It is this emission that would be responsible for the rise in fluorescence seen in vivo (F_V). A prediction of this hypothesis is that cells in a highly fluorescent state will exhibit a new fluorescence decay component with a lifetime around 15–20 ns, corresponding to the delayed fluorescence after charge recombination. Such a long-lived component (~ 18 ns) was observed in isolated *H. mobilis* membrane fragments after treatment with dithionite (Kleinherenbrink et al. 1994). We tested this hypothesis using TCSPC.

Fresh *H. modesticaldum* culture was anoxically loaded into a sealed cuvet and analyzed by the TCSPC technique. Emission was collected at wavelengths in the range of 790–860 nm, which should correspond to emission from BChl g. The vast majority ($>99.9\%$) of the fluorescence in cells decayed with a time constant of ~ 20 ps (Fig. 6a; Table 1), which is the trapping time in the HbRC from this species (Sarrou et al. 2012). The sum of the long-lived components (>1 ns) is less than 0.1%, likely due to some free pigments. In contrast, after addition of dithionite to the

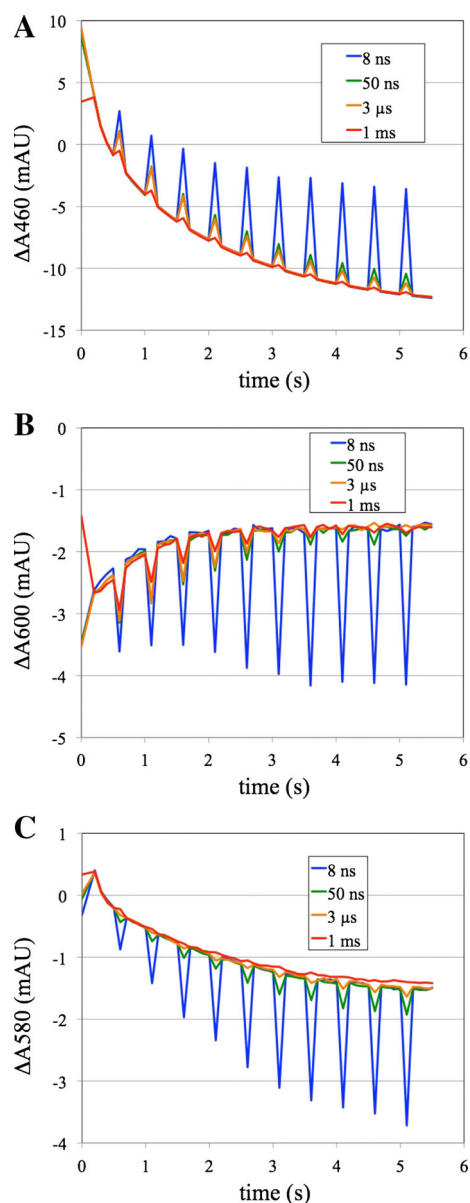


Fig. 4 Induction of rapidly recombining state by illumination of untreated *H. modesticaldum* cells. Cells in anoxic medium were illuminated with laser diode ($400 \mu\text{mol photons m}^{-2} \text{s}^{-1}$ centered at 690 nm), starting at 100 ms after the first pump-probe measurement. During each time course, a saturating red laser pump flash was fired every 500 ms followed by a probe flash at 460 nm (a), 600 nm (b), or 580 nm (c) after a delay of 8 ns (blue), 50 ns (green), 3 μs (orange), or 1 ms (red). Between pump flashes, absorption changes were measured every 100 ms with the same probe flash

cells, a significant increase of long-lived fluorescence decay is observed. The result worth noting is the resolution of a new long-lived component of 15–20 ns, which accounted for 0.5–0.6 % of the total amplitude (Fig. 6a; Table 1). This component is practically nonexistent (≤ 0.003 %) in cells before dithionite treatment. This time constant is very similar to that of the back-reaction measured by pump-probe spectroscopy (e.g. Fig. 3a) and seen

in dithionite-treated membranes (Kleinherenbrink et al. 1994). The dithionite-treated cells also exhibited a ~ 10 -fold increase in the other slower components of 600–900 ps and ~ 3 ns (see Table 1). The reason for the slowing of the trapping time from 25 to 36 ps is unclear at this time, but it may be due to destabilization of the initial charge-separated state in the presence of the reduced acceptor (i.e., $\text{RC}^*\text{X}^- \rightarrow \text{P}^+\text{A}_0^-\text{X}^-$ would be slower than $\text{RC}^*\text{X} \rightarrow \text{P}^+\text{A}_0^-\text{X}$). Note that if one sums the product of the amplitudes and lifetimes, it is possible to predict an increase in steady-state emission of about five to sixfold.

The DAS of these decay components from cells without and with dithionite are shown in Fig. 6b, c, respectively. The emission spectrum of the slowest component (18 ns) resembles that of the BChl *g* antenna system in the HbRC, peaking at ~ 810 nm (Fig. 6c). It is only slightly red-shifted compared to the DAS of the trapping component (20–40 ps). Under the same conditions, we also see an increase of the steady-state fluorescence emission in the 790–830 nm region by ~ 3 –4-fold, depending upon the excitation wavelength (Fig. S8). Thus, we conclude that the 18-ns fluorescence decay represents delayed fluorescence after charge recombination of the $\text{P}_{800}^+\text{A}_0^-$ state, and the large increase in this component (>100 -fold increase after dithionite treatment) is the origin of the higher steady-state fluorescence, as seen previously with dithionite-treated membranes from *H. mobilis* (Kleinherenbrink et al. 1994).

Discussion

In an earlier publication in which variable fluorescence from living heliobacteria was first reported (Collins et al. 2010), it was hypothesized that this phenomenon arose from HbRCs that were undergoing charge recombination from $\text{P}_{800}^+\text{A}_0^-$ after reduction of the acceptor side. Here, we have tested that hypothesis using a series of time-resolved absorption and fluorescence studies on living cells of *H. modesticaldum*. We have found that the ability of P_{800} in the HbRC to be stably photobleached (i.e. persisting for $>200 \mu\text{s}$) correlates inversely with the variable fluorescence emitted by the culture under a wide variety of conditions. Situations that tend to result in reduction of the electron acceptor pool (e.g. treatment of cells with dithionite and PMS; see Fig. S6) also lead to less stable P_{800} photobleaching and to variable fluorescence that rises earlier and to higher levels. In contrast, addition of stigmatellin, which inhibits re-reduction of the mobile cyt c_{553} and thereby re-reduction of P_{800}^+ , has the opposite effect (e.g. Fig. S5). In the ns timescale, we found that illumination of cells for a few seconds with bright light could put most of the HbRCs into a state that underwent rapid charge recombination from $\text{P}_{800}^+\text{A}_0^-$. The fact that this process was accelerated by addition of dithionite,

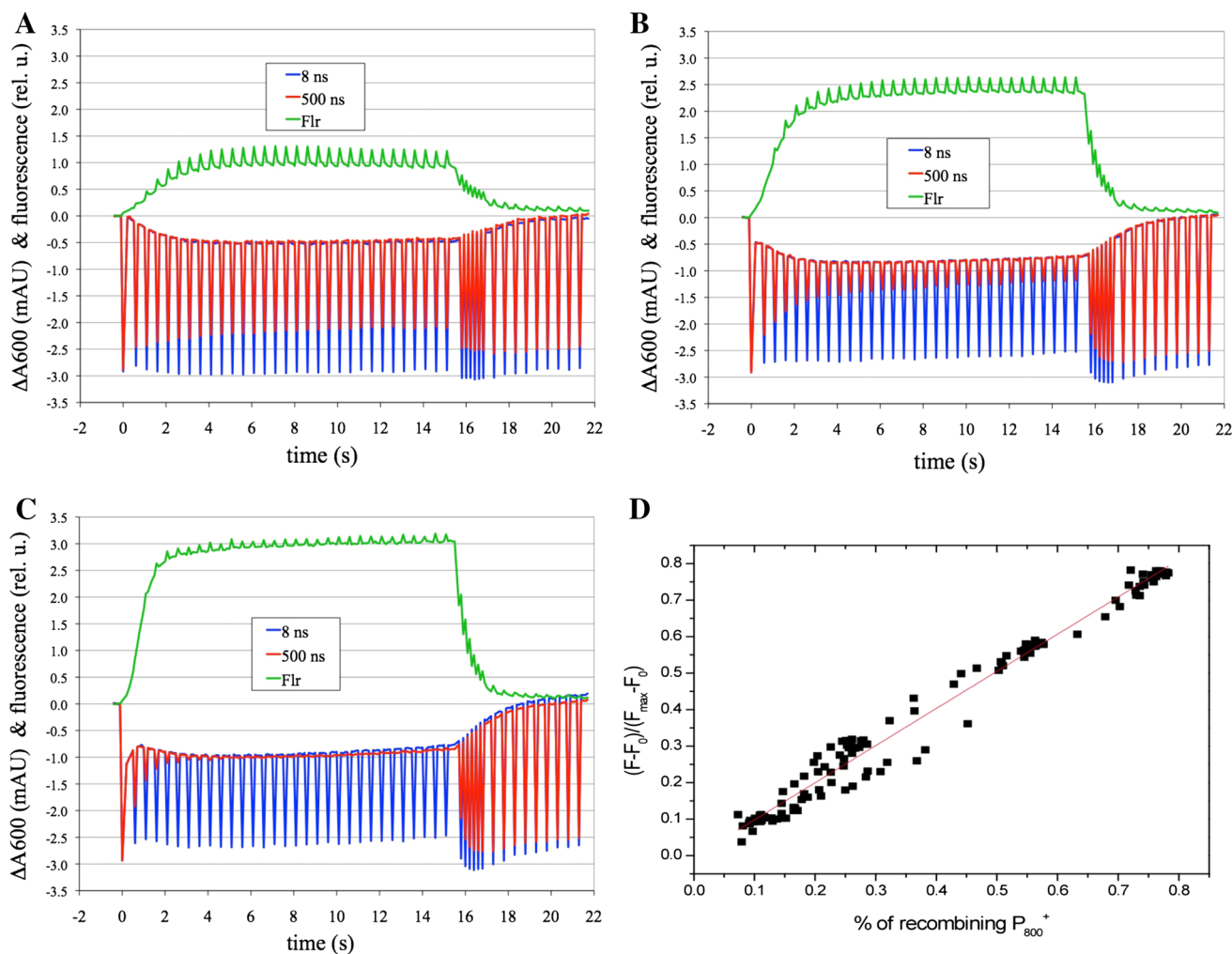


Fig. 5 Time course of fluorescence rise and the loss of stable P_{800} photobleaching Cells were treated essentially the same as in the legend to Fig. 4, except that illumination persisted for 15 s and spectroscopic changes were monitored for 5 s after illumination was terminated. (The first five flashes after the actinic light was extinguished were spaced every 200 ms to observe the recovery phase.) Actinic photon flux was 50 $\mu\text{mol m}^{-2} \text{s}^{-1}$ (a), 200 $\mu\text{mol m}^{-2} \text{s}^{-1}$ (b), or 500 $\mu\text{mol m}^{-2} \text{s}^{-1}$ (c). The stability of P_{800} photobleaching induced by the probe pulse was assessed by probe flashes 8 ns (blue) and 500 ns (red) after the 6-ns pump flash. Fluorescence emission (>780 nm) was measured using an identical protocol, except that a probe flash at 420 nm was used to excite the

sample, and fluorescence was collected through long-pass optical filters. *Note* that the pump flash induces a transient fluorescence increase; the excitation flash followed the pump flash after a 10-ns delay. **d** Plotted the fraction of back-reacting RCs versus the variable fluorescence measured at the same time point on the 3 different curves. (The maximal fluorescence was estimated from the fluorescence obtained using an actinic intensity of 1,700 $\mu\text{mol m}^{-2} \text{s}^{-1}$, as no increase in fluorescence was observed after the laser pump flashes in this case, indicating that saturation had been achieved; not shown). The data was fit to a linear equation (slope = 1.018 ± 0.013 and intercept = -0.004 ± 0.006) with good agreement ($R^2 = 0.979$)

but was not dependent upon it, argues that this phenomenon is a natural consequence of limitations in electron flow within the heliobacterial cell. Use of an instrument that could measure fluorescence and transient absorption changes in the ns timescale demonstrated a strong linear correlation between variable fluorescence and the fraction of HbRCs that were undergoing charge recombination from $P_{800}^+A_0^-$. Time-resolved fluorescence studies in the ps-ns timescale showed that addition of dithionite to cells led to the appearance of a long-lived component of fluorescence decay (~ 18 ns), which could account for more than 0.5 %

of the decay. In all cases, the vast majority of the fluorescence (>98 %) decayed with a time constant of ≤ 50 ps, and was consistent with photochemical trapping. The DAS of trapping and delayed fluorescence were very similar, indicating that both were emitted from excited HbRC antenna pigments. The steady-state fluorescence emission spectra from cells had a similar spectral shape (Fig. S8), and also increased with addition of dithionite, providing further support for the idea that the increase of fluorescence emission was largely due to the increase of the 18-ns component assigned to emission after charge recombination.

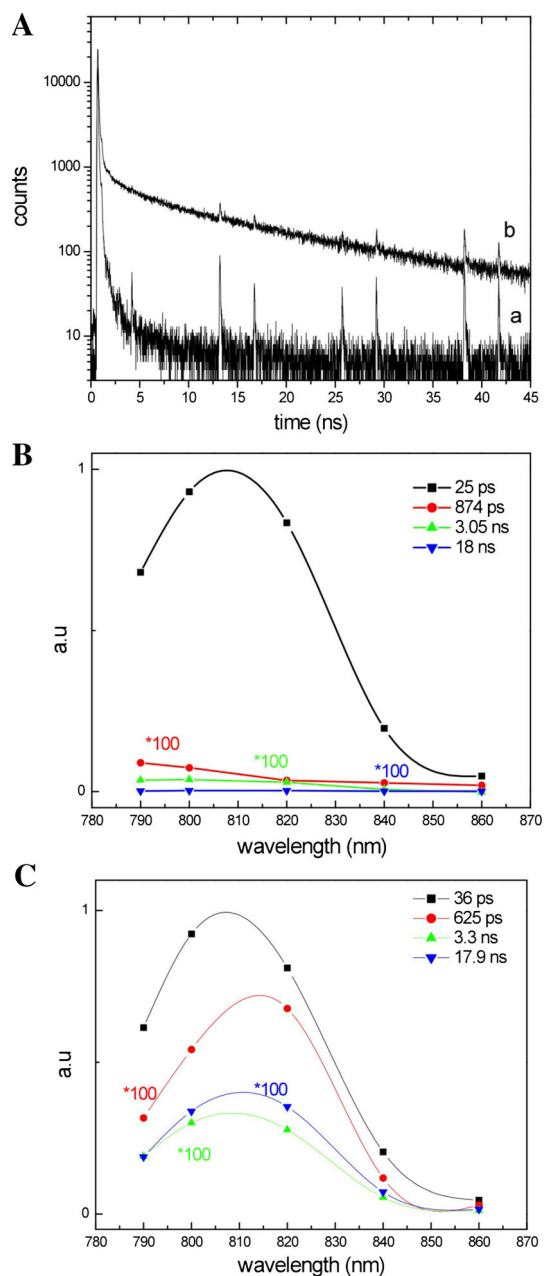


Fig. 6 Time-resolved fluorescence analysis in live heliobacterial cells. **a** Comparison of fluorescence decay kinetics of *H. modesticaldum* cells recorded at 810 nm on the 50-ns timescale without (black) and with dithionite (red). (Periodic spikes are due to the incomplete removal of the rejected pulses from the pulse selector). The DAS of fluorescence decay components, from global fitting of kinetics between 790 and 860 nm on the 50-ns timescale are shown for living cells without (b) and with (c) addition of 50 mM dithionite

Mechanism of delayed fluorescence emission by the HbRC

We have identified the state that undergoes charge recombination, thereby leading to fluorescence emission, as $P_{800}^+A_0^-$. The species that correlates with the rise of

variable fluorescence has a decay constant of ~ 18 ns. This time constant and the transient difference spectrum (Fig. 3) are both consistent with this species being $P_{800}^+A_0^-$. What is unclear at this point is the exact identity of the cofactor ‘X’ that is reduced, thereby blocking forward ET from A_0 . At this point, the role of the menaquinone found in the HbRC is controversial, as discussed in the Introduction. If MQ is not used as an intermediate in ET between A_0 and F_X , then the state undergoing back-reaction after excitation would be $P_{800}F_X^-$. If MQ were used as an obligatory intermediate in ET from A_0 to F_X , then the state undergoing back-reaction after excitation would be $P_{800}MQ^-$. Although we cannot exclude between those two possibilities based on the data reported here, we found that *H. modesticaldum* HbRCs almost completely lacking MQ behaved identically to HbRCs containing MQ, in terms of charge separation, kinetics of forward ET from A_0 and back-reaction from F_X ; moreover, the addition of MQ had no discernable effect (Chauvet et al. 2013). Kleinherenbrink et al. (Kleinherenbrink et al. 1993) had previously found no effect upon forward ET after depletion of menaquinone from membranes of *H. chlorum*. We have also found that addition of dithionite to the purified core HbRC results in reduction of F_X without any sign of a semiquinone radical, leading to a state that is unable to stably photobleach P_{800} ; this state is quickly reversed by brief exposure to air (Cowgill et al. manuscript in preparation). Thus, we think it most likely that the rapidly recombining state responsible for the delayed fluorescence is one in which the F_X cluster is reduced.

Delayed fluorescence has been seen before in type 1 RCs. It was observed in PS1 particles and PS1-containing membranes that had been illuminated in the presence of dithionite (Ikegami 1976; Tripathy et al. 1984; Kleinherenbrink et al. 1994). Similar increases in steady-state fluorescence was seen in heliobacterial membranes upon reduction by dithionite (Kleinherenbrink et al. 1994). In membranes containing either PS1 or the HbRC, the increase of steady-state fluorescence was explained by the rise of a long-lived (~ 15 – 50 ns) component of fluorescence decay, attributed to delayed fluorescence after charge recombination from the $P^+A_0^-$ state (Kleinherenbrink et al. 1994). What we have observed here in illuminated heliobacterial cells is very likely to be the same phenomenon, as it has similar characteristics.

An important issue that we have left unaddressed so far is the intrinsic yield of delayed fluorescence. We predict that there are multiple fates possible after excitation of an HbRC in the $P_{800}F_X^-$ state. While, the yield of trapping may be slightly reduced in this state, the major effect on trapping is to reduce its rate from 25 to 36 ps (Table 1). This is likely due to the negative charge on F_X^- raising the energy of the initial charge-separated state (i.e., the energy of

Table 1 Fluorescence decay components in live *H. modesticaldum* cells obtained on a 50-ns timescale, obtained from global analysis using a sum of exponential decays model

| Sample | τ_1 (%) | τ_2 (%) | τ_3 (%) | τ_4 (%) | χ^2 |
|--------------------|-----------------|-----------------|-------------------|-------------------|----------|
| Cells | 25 ps (99.91 %) | 875 ps (0.06 %) | 3.05 ns (0.021 %) | 18.0 ns (0.003 %) | 1.37 |
| Cells + dithionite | 36 ps (98.48 %) | 625 ps (0.69 %) | 3.32 ns (0.37 %) | 17.9 ns (0.54 %) | 1.03 |

$P_{800}^+A_0^-F_X^-$ is higher than that of $P_{800}^+A_0^-F_X$. Once, the $P_{800}^+A_0^-F_X^-$ state has been formed, there are four possible pathways to consider: (1) internal conversion to the ground state ($P_{800}F_X^-$); (2) charge recombination of $P_{800}^+A_0^-$ to the excited triplet state (${}^3P_{800}F_X^-$); (3) charge recombination to the excited singlet state ($P_{800}^*F_X^-$); and (4) forward ET to an alternate acceptor, Z (yielding $P_{800}^+F_X^-Z^-$) or perhaps $P_{800}^+F_XZ^{2-}$). Since, the lifetime of P_{800}^+ largely matches that of A_0^- when cells are in the back-reacting state (Fig. 4), it appears that the fourth hypothetical pathway would represent a minor pathway. Thus, we will focus on charge recombination. Only the third pathway would lead to fluorescence emission, and this would be in competition with the first two pathways.

In order to simplify the analysis, we consider a two-state model: the excited state (Ant/RC*) and the initial charge-separated state ($P_{800}^+A_0^-$). This model is discussed in greater detail in the Supplemental information (see Fig. S9). We will ignore the ~ 3 -ns fluorescence decay component, as this is almost surely due to a small amount of uncoupled pigments; we will also assume that the intrinsic fluorescence emission rate is roughly 3 ns^{-1} . We thus take into account the 25- and 875-ps lifetimes for the sample under ambient redox conditions (i.e. F_X oxidized), and the 36-ps and the 18-ns components for the dithionite-treated sample (i.e. F_X reduced). The lifetime of 875 ps is close to the estimated transfer time from A_0^- to F_X , and would thus represent effective “exit” from the two-state system. Observation of this component in the fluorescence emission decay implies that interconversion of the two states occurs on a time scale comparable to excited state decay. The same argument can be applied to the case in which F_X is reduced, with the 18-ns component representing overall conversion of the charge-separated state and excited state to a non-fluorescent one. The amplitude of this component provides an estimate for repopulation of the excited singlet state from the charge-separated state. In the case of F_X oxidized, to reproduce an amplitude of $\sim 0.06 \%$ for the 875-ps component with a charge separation rate from the antenna of about 40 ns^{-1} , and a depopulation of the charge-separated state by forward ET of 1.2 ns^{-1} , the rate of recombination to the emitting state (k_{CR} in the model; Fig. S9A) must be $\sim 0.02 \text{ ns}^{-1}$ (i.e. $\sim 2,000$ -fold slower than photochemistry). When F_X is reduced, the amplitude of the slower phase (18-ns in this case) increases ninefold

(Table 1). Considering a charge separation rate of 28 ns^{-1} (due to the slower decay observed in the measurements) and a non-radiative depopulation of the charge separated state F_X of 0.05 ns^{-1} , the rate of repopulation of the antenna excited state from $P_{800}^+A_0^-$ must be $\sim 0.16 \text{ ns}^{-1}$ (i.e. ~ 8 times faster than when F_X is oxidized). Thus, the pseudo-equilibrium between Ant/RC* and $P_{800}^+A_0^-$ governed by k_{CS}/k_{CR} would be $\sim 2,000$ with F_X oxidized and ~ 175 with F_X reduced, which is perhaps unsurprising given the extra negative charge on F_X in the latter case. One can thus estimate the ratio of non-radiative to radiative decay from the equilibrated two-state system to be $(k_{out}/k_f) \cdot (k_{CS}/k_{CR})$, which would be 26 when F_X is reduced. A numerical simulation using these rate constants, which takes into account decay from the pre-equilibrated system (where fluorescence emission is favored), gives a ratio of ~ 20 . Using these rate constants, we also calculate that fluorescence emission would be ~ 5 -fold higher when F_X is reduced than when it is oxidized, which agrees fairly well with our data. These numbers should not be taken too seriously, as these are only rough estimates, but we are likely to be close to the actual rates, as the numbers calculated from the numerical simulation do not depend very sensitively on the rate constants used.

Our data seem to suggest that RC triplet formation at room temperature is negligible, as we failed to observe spectral features characteristic of BChl *g* triplet–triplet absorption. Thus, we tentatively suggest that the rate of internal conversion to the ground state is much higher than the rate of conversion to the triplet state. The ${}^3P_{800}$ triplet state has been detected at low temperatures in membranes from *H. chlorum*, however, and its formation was shown to be dependent on the redox state of the acceptor side (Vrieze et al. 1998). It is possible that the yields of the different pathways after formation of the charge-separated state in the presence of F_X^- are somewhat temperature dependent. Further work will be required to resolve these issues.

Why does the acceptor pool become limiting?

One of the consequences of our conclusion about the origin of heliobacterial variable fluorescence is the requirement that the in vivo pool of electron acceptors becomes exhausted before the pool of electron donors. We know this is the case, because inhibition of the cyt *b_{6c}* complex with

stigmatellin results in a decrease in fluorescence (Collins et al. 2010); see Fig. S5). This also implies that the pool of electron donors to the RC extends beyond the pool of cyt c_{553} . This is presumably because there is no (stable) charge separation in RCs with oxidized P_{800} , and charge separation must precede charge recombination. Also, addition of dithionite (with the mediator PMS) has the effect of hastening the rise and increasing the extent of fluorescence after illumination commences. We interpret this to mean that the addition of exogenous low-potential reductant has the effect of reducing cellular electron acceptors, rather than the acceptor side of the HbRC itself. If the latter had occurred, then one would expect to see an immediate rise in fluorescence without the need for pre-illumination.

However, we must say that this conclusion is rather unexpected. To our knowledge, the only electron donor to the HbRC is the mobile, membrane-attached cyt c_{553} . In contrast, there are likely several primary and secondary electron acceptors, if one considers all the ferredoxins and NAD(P) pools that are in redox equilibrium with the immediate electron acceptor(s) of the HbRC. Moreover, there are several electron sinks in the cell, including all the anabolic pathways that require reducing power. The major input of electrons into the electron acceptor pool is likely the oxidation of pyruvate (the major carbon/electron source in the medium) via the pyruvate:ferredoxin oxidoreductase, and these cells were grown on pyruvate. At this point, we simply do not know the relative fluxes of the various pathways to and from the cellular electron acceptor pool. However, we can say that some light-independent step(s) must become limiting when the HbRC is driven by strong continuous light. Given that inhibition of the cyt b_6c complex with stigmatellin results in a decrease in fluorescence, we can rule out this enzyme as the weak link in the chain. If we consider the other enzymes likely to be involved in cyclic electron flow in heliobacteria, possible candidates for the rate-limiting steps include FNR (ferredoxin:NAD oxidoreductase) and the NAD(P)H:menaquinone oxidoreductase. A limitation by either of these enzymes would result in a back-up of electrons in the acceptor pool.

Finally, it is worth noting that all the studies shown here were performed at room temperature (23–25 °C), but the organism was grown at 45–48 °C. Thus, one might well ask if the limitation in electron flow was due to a retardation of specific steps due to the lowered temperature. This does not appear to be the case, as it has already been shown that fluorescence actually rises faster as the temperature rises from 20 to 48 °C in *H. modesticaldum* (Collins et al. 2010). Also, electron donation from the membrane-attached cyt c_{553} to P_{800}^+ is very temperature dependent, slowing as the temperature falls (Oh-oka et al. 2002; Kashey et al. submitted for publication). One might also expect that enzymes using quinones as substrates may

have lower steady-state rates, if diffusion of MQ in the membrane becomes markedly slower at lowered temperature. In the cyclic electron transport pathway, one might therefore expect to see retardation of the cyt b_6c complex and the NAD(P)H:menaquinone oxidoreductase. Given that we know that slowing of ET from the cyt b_6c complex via the mobile cyt c will result in lowered fluorescence (due to accumulation of closed RCs), we therefore think it unlikely that the lowered temperature is a cause, direct or indirect, of the variable fluorescence phenomenon described here, although it certainly modulates the kinetics of its rise and fall.

Acknowledgments Much of this work was performed while KR was visiting the group of Francis-André Wollman at the Institut de Biologie Physico-Chimique (Paris) as a J. William Fulbright Scholar. KR is grateful to the FAW and the CNRS, as well as the Fulbright program, for their support during his stay in Paris. Work performed in KR's laboratory at ASU was supported by the Division of Chemical Sciences, Geosciences, and Biosciences, Office of Basic Energy Sciences of the U.S. Department of Energy through Grant DE-SC0010575.

References

- Albert I, Rutherford AW, Grav H, Kellermann J, Michel H (1998) The 18-kDa cytochrome c_{553} from *Helicobacterium gestii*: gene sequence and characterization of the mature protein. *Biochemistry* 37(25):9001–9008
- Amesz J (1995) The antenna-reaction center complex of heliobacteria. *Advances in Photosynthesis 2 (Anoxygenic Photosynthetic Bacteria)*:687–697
- Béal D, Rappaport F, Joliot P (1999) A new high-sensitivity 10-ns time-resolution spectrophotometric technique adapted to in vivo analysis of the photosynthetic apparatus. *Rev Sci Instrum* 70:202–207
- Bowes JM, Crofts AR (1980) Binary oscillations in the rate of reoxidation of the primary acceptor of Photosystem II. *Biochim Biophys Acta* 590(3):373–384
- Brettel K, Leibl W, Liebl U (1998) Electron transfer in the heliobacterial reaction center: evidence against a quinone-type electron acceptor functioning analogous to A1 in Photosystem I. *Biochim Biophys Acta* 1363(3):175–181
- Broess K, Trinkunas G, van der Weij-de Wit CD, Dekker JP, van Hoek A, van Amerongen H (2006) Excitation energy transfer and charge separation in Photosystem II membranes revisited. *Biophys J* 91(10):3776–3786
- Buttler W (1978) Energy distribution in the photochemical apparatus of photosynthesis. *Ann Rev Plant Physiol* 29:345–378
- Byrdin M, Rimke I, Schlodder E, Stehlik D, Roelofs TA (2000) Decay kinetics and quantum yields of fluorescence in Photosystem I from *Synechococcus elongatus* with P_{700} in the reduced and oxidized state: Are the kinetics of excited state decay trap-limited or transfer-limited? *Biophys J* 79(2):992–1007
- Caffari S, Broess K, Croce R, van Amerongen H (2011) Excitation energy transfer and trapping in higher plant Photosystem II complexes with different antenna sizes. *Biophys J* 100(9):2094–2103
- Chauvet A, Sarrou J, Lin S, Romberger SP, Golbeck JH, Savikhin S, Redding KE (2013) Temporal and spectral characterization of

- the photosynthetic reaction center from *Heliobacterium modesticaldum*. *Photosynth Res* 116(1):1–9
- Clayton RK (1965) Characteristics of fluorescence and delayed light emission from green photosynthetic bacteria and algae. *J Gen Physiol* 48:633–646
- Clayton RK (1967) An analysis of the relations between fluorescence and photochemistry during photosynthesis. *J Theor Biol* 14(2):173–186
- Collins AM, Redding KE, Blankenship RE (2010) Modulation of fluorescence in *Heliobacterium modesticaldum* cells. *Photosynth Res* 104(2–3):283–292
- Ducluzeau AL, Chenu E, Capowiez L, Baymann F (2008) The Rieske/cytochrome *b* complex of Heliobacteria. *Biochim Biophys Acta* 1777(9):1140–1146
- Duysens LN (1978) Transfer and trapping of excitation energy in Photosystem II. *Ciba Found Symp* 61:323–340
- Engelmann EC, Zucchelli G, Garlaschi FM, Casazza AP, Jennings RC (2005) The effect of outer antenna complexes on the photochemical trapping rate in barley thylakoid Photosystem II. *Biochim Biophys Acta* 1706(3):276–286
- Engelmann E, Zucchelli G, Casazza AP, Brogioli D, Garlaschi FM, Jennings RC (2006) Influence of the Photosystem I-light harvesting complex I antenna domains on fluorescence decay. *Biochemistry* 45(22):6947–6955
- Galka P, Santabarbara S, Khuong TT, Degand H, Morsomme P, Jennings RC, Boekema EJ, Caffarri S (2012) Functional analyses of the plant Photosystem I-light-harvesting complex II super-complex reveal that light-harvesting complex II loosely bound to Photosystem II is a very efficient antenna for Photosystem I in state II. *Plant Cell* 24(7):2963–2978
- Giera W, Ramesh VM, Webber AN, van Stokkum I, van Grondelle R, Gibasiewicz K (2010) Effect of the P₇₀₀ pre-oxidation and point mutations near A₀ on the reversibility of the primary charge separation in Photosystem I from *Chlamydomonas reinhardtii*. *Biochim Biophys Acta* 1797(1):106–112
- Gobets B, van Grondelle R (2001) Energy transfer and trapping in Photosystem I. *Biochim Biophys Acta* 1507(1–3):80–99
- Guergova-Kuras M, Boudreaux B, Joliot A, Joliot P, Redding K (2001) Evidence for two active branches for electron transfer in Photosystem I. *Proc Natl Acad Sci USA* 98(8):4437–4442
- Hastings G, Kleinherenbrink FA, Lin S, Blankenship RE (1994) Time-resolved fluorescence and absorption spectroscopy of Photosystem I. *Biochemistry* 33(11):3185–3192
- Heinzel M, Shen G, Agalarov R, Golbeck JH (2005) Resolution and reconstitution of a bound Fe–S protein from the photosynthetic reaction center of *Heliobacterium modesticaldum*. *Biochemistry* 44(29):9950–9960
- Heinzel M, Agalarov R, Svensen N, Krebs C, Golbeck JH (2006) Identification of F_X in the heliobacterial reaction center as a [4Fe–4S] cluster with an S = 3/2 ground spin state. *Biochemistry* 45(21):6756–6764
- Heinzel M, Shen G, Golbeck JH (2007) Identification and characterization of PshB, the dicluster ferredoxin that harbors the terminal electron acceptors F(A) and F(B) in *Heliobacterium modesticaldum*. *Biochemistry* 46(9):2530–2536
- Hiraishi A (1989) Occurrence of menaquinone is the sole isoprenoid quinone in the photosynthetic bacterium *Heliobacterium chlorum*. *Arch Microbiol* 151:378–379
- Hodges M, Moya I (1986) Time-resolved chlorophyll fluorescence studies of photosynthetic membranes: resolution and characterization of four kinetic components. *Biochim Biophys Acta* 849:193–202
- Hohmann-Mariotti MF, Blankenship RE (2007) Variable fluorescence in green sulfur bacteria. *Biochim Biophys Acta* 1767(1):106–113
- Holzwarth AR, Wendler J, Haehnel W (1985) Time-resolved picosecond fluorescence spectra of the antenna chlorophylls in *Chlorella vulgaris*. Resolution of Photosystem I fluorescence. *Biochim Biophys Acta* 807:155–167
- Holzwarth AR, Muller MG, Niklas J, Lubitz W (2006) Ultrafast transient absorption studies on Photosystem I reaction centers from *Chlamydomonas reinhardtii*. 2 Mutations near the P₇₀₀ reaction center chlorophylls provide new insight into the nature of the primary electron donor. *Biophys J* 90(2):552–565
- Ihalainen JA, van Stokkum IH, Gibasiewicz K, Germano M, van Grondelle R, Dekker JP (2005) Kinetics of excitation trapping in intact Photosystem I of *Chlamydomonas reinhardtii* and *Arabidopsis thaliana*. *Biochim Biophys Acta* 1706(3):267–275
- Ikegami I (1976) Fluorescence changes related in the primary photochemical reaction in the P₇₀₀-enriched particles isolated from spinach chloroplasts. *Biochim Biophys Acta* 449(2):245–258
- Jagannathan B, Golbeck JH (2009a) Breaking biological symmetry in membrane proteins: the asymmetrical orientation of PsaC on the pseudo-C₂ symmetric Photosystem I core. *Cell Mol Life Sci* 66(7):1257–1270
- Jagannathan B, Golbeck JH (2009b) Understanding of the binding interface between PsaC and the PsaA/PsaB heterodimer in Photosystem I. *Biochemistry* 48(23):5405–5416
- Jennings RC, Zucchelli G, Santabarbara S (2013) Photochemical trapping heterogeneity as a function of wavelength, in plant Photosystem I (PSI-LHCI). *Biochim Biophys Acta* 1827(6):779–785
- Kleinherenbrink FAM, Aartsma TJ, Amez J (1991) Charge separation and formation of bacteriochlorophyll triplets in *Heliobacterium chlorum*. *Biochim Biophys Acta* 1057(3):346–352
- Kleinherenbrink FA, Ikegami I, Hiraishi A, Otte SCM, Amez J (1993) Electron transfer in menaquinone-depleted membranes of *Heliobacterium chlorum*. *Biochim Biophys Acta* 1142:69–73
- Kleinherenbrink FAM, Hastings G, Wittmershaus BP, Blankenship RE (1994) Delayed fluorescence from Fe–S Type photosynthetic reaction centers at low redox potential. *Biochem* 33(10):3096–3105
- Kramer DM, Schoepp B, Liebl U, Nitschke W (1997) Cyclic electron transfer in *Heliobacillus mobilis* involving a menaquinol-oxidizing cytochrome *bc* complex and an RCI-type reaction center. *Biochemistry* 36(14):4203–4211
- Liddell PA, Gervaldo M, Bridgewater JW, Keirstead AE, Lin S, Moore TA, Moore AL, Gust D (2008) Porphyrin-based hole conducting electropolymer. *Chem Mater* 20:135–142
- Lin S, Chiou HC, Blankenship RE (1995) Secondary electron transfer processes in membranes of *Heliobacillus mobilis*. *Biochemistry* 34(39):12761–12767
- Miloslavina Y, Szczepaniak M, Muller MG, Sander J, Nowaczyk M, Rogner M, Holzwarth AR (2006) Charge separation kinetics in intact Photosystem II core particles is trap-limited. A picosecond fluorescence study. *Biochemistry* 45(7):2436–2442
- Miyamoto R, Mino H, Kondo T, Itoh S, Oh-Oka H (2008) An electron spin-polarized signal of the P₈₀₀⁺A₁(Q)[−] state in the homodimeric reaction center core complex of *Heliobacterium modesticaldum*. *Biochemistry* 47(15):4386–4393
- Moya I, Hodges M, Barbet J-C (1986) Modification of room-temperature picosecond chlorophyll fluorescence kinetics in green algae by Photosystem II trap closure. *FEBS Lett* 198:256–262
- Muhiuddin IP, Rigby SE, Evans MC, Amez J, Heathcote P (1999) ENDOR and special TRIPLE resonance spectroscopy of photoaccumulated semiquinone electron acceptors in the reaction centers of green sulfur bacteria and heliobacteria. *Biochemistry* 38(22):7159–7167
- Müller MG, Niklas J, Lubitz W, Holzwarth AR (2003) Ultrafast transient absorption studies on Photosystem I reaction centers from *Chlamydomonas reinhardtii* I. A new interpretation of the energy trapping and early electron transfer steps in Photosystem I. *Biophys J* 85(6):3899–3922

- Müller MG, Slavov C, Luthra R, Redding KE, Holzwarth AR (2010) Independent initiation of primary electron transfer in the two branches of the Photosystem I reaction center. *Proc Natl Acad Sci USA* 107(9):4123–4128
- Neerken S, Amesz J (2001) The antenna reaction center complex of heliobacteria: composition, energy conversion and electron transfer. *Biochim Biophys Acta* 1507(1–3):278–290
- Nitschke W, Liebl U, Matsuura K, Kramer DM (1995) Membrane-bound c-type cytochromes in *Heliobacillus mobilis*. In vivo study of the hemes involved in electron donation to the photosynthetic reaction center. *Biochemistry* 34(37):11831–11839
- Oh-oka H, Iwaki M, Itoh S (2002) Electron donation from membrane-bound cytochrome *c* to the photosynthetic reaction center in whole cells and isolated membranes of *Heliobacterium gestii*. *Photosynth Res* 71(1–2):137–147
- Parrett KG, Mehari T, Warren PG, Golbeck JH (1989) Purification and properties of the intact P-700 and F_X -containing Photosystem I core protein. *Biochim Biophys Acta* 973(2):324–332
- Rappaport F, Diner BA, Redding K (2006) Optical measurements of secondary electron transfer in Photosystem I. In: Golbeck J (ed) Photosystem I: the plastocyanin:ferredoxin oxidoreductase in photosynthesis. Kluwer Academic, Dordrecht, pp 223–244
- Reed DW, Zankel KL, Clayton RK (1969) The effect of redox potential on P_{870} fluorescence in reaction centers from *Rhodospseudomonas spheroides*. *Proc Natl Acad Sci USA* 63(1):42–46
- Roelofs TA, Lee CH, Holzwarth AR (1992) Global target analysis of picosecond chlorophyll fluorescence kinetics from pea chloroplasts: a new approach to the characterization of the primary processes in Photosystem II alpha- and beta-units. *Biophys J* 61(5):1147–1163
- Romberger SP, Golbeck JH (2012) The F_X iron-sulfur cluster serves as the terminal bound electron acceptor in heliobacterial reaction centers. *Photosynth Res* 111:285–290
- Romberger SP, Castro C, Sun Y, Golbeck JH (2010) Identification and characterization of PshBII, a second F_A/F_B -containing polypeptide in the photosynthetic reaction center of *Heliobacterium modesticaldum*. *Photosynth Res* 104(2–3):293–303
- Samson G, Prasil O, Yaakoub B (1999) Photochemical and thermal phases of chlorophyll *a* fluorescence. *Photosynthetica* 37(2):163–182
- Santabarbara S, Heathcote P, Evans MC (2005) Modelling of the electron transfer reactions in Photosystem I by electron tunneling theory: the phyloquinones bound to the PsaA and the PsaB reaction centre subunits of PS I are almost isoenergetic to the iron-sulfur cluster F_X . *Biochim Biophys Acta* 1708(3):283–310
- Sarrou I, Khan Z, Cowgill J, Lin S, Brune D, Romberger S, Golbeck JH, Redding KE (2012) Purification of the photosynthetic reaction center from *Heliobacterium modesticaldum*. *Photosynth Res* 111(3):291–302
- Schatz GH, Brock H, Holzwarth AR (1988) Kinetic and energetic model for the primary processes in Photosystem II. *Biophys J* 54(3):397–405
- Sétif P, Brettel K (1993) Forward electron transfer from phyloquinone A_1 to iron-sulfur centers in spinach Photosystem I. *Biochem* 32(31):7846–7854
- Slavov C, Ballottari M, Morosinotto T, Bassi R, Holzwarth AR (2008) Trap-limited charge separation kinetics in higher plant Photosystem I complexes. *Biophys J* 94(9):3601–3612
- Tripathy BC, Draheim JE, Anderson GP, Gross EL (1984) Variable fluorescence of Photosystem I particles and its application to the study of the structure and function of Photosystem I. *Arch Biochem Biophys* 235(2):449–460
- van der Est A, Hager-Braun C, Leibl W, Hauska G, Stehlik D (1998) Transient electron paramagnetic resonance spectroscopy on green-sulfur bacteria and heliobacteria at two microwave frequencies. *Biochim Biophys Acta* 1409(2):87–98
- van Grondelle R, Holmes NG, Rademaker H, Duysens LN (1978) Bacteriochlorophyll fluorescence of purple bacteria at low redox potentials. The relationship between reaction center triplet yield and the emission yield. *Biochim Biophys Acta* 503(1):10–25
- Vrieze J, Van de Meent EJ, Hoff AJ (1998) Triplet properties and interactions of the primary electron donor and antenna chromophores in membranes of *Heliobacterium chlorum*, studied with ADMR spectroscopy. *Biochemistry* 37(42):14900–14909
- White NTH, Beddard GS, Thorne JRG, Feehan TM, Keyes TE, Heathcote P (1996) Primary charge separation and energy transfer in the Photosystem I reaction center of higher plants. *J Phys Chem* 100(29):12086–12099
- Wientjes E, van Stokkum IH, van Amerongen H, Croce R (2011) The role of the individual LhcAs in Photosystem I excitation energy trapping. *Biophys J* 101(3):745–754
- Zankel KL, Reed DW, Clayton RK (1968) Fluorescence and photochemical quenching in photosynthetic reaction centers. *Proc Natl Acad Sci USA* 61(4):1243–1249